Behavior of a coal pillar prone to burst in the southern Appalachian Basin of the United States

Anthony Iannacchione
US Department of the Interior, Bureau of Mines, Pittsburg, Pa., USA

ABSTRACT: One of the more pressing engineering problems for deep longwall mines in the Southern Appalachian Basin is to design longwall systems that will eliminate catastrophic coal pillar failure from the working environment. The purpose of this study is to quantify the behavior of a particular size abutment pillar prone to burst or bump. Because the 24.4-m (80-ft) square abutment study pillar is within the pillar size commonly used in this region, understanding the behavior of this pillar should aid in future efforts to design optimum mining strategies. This research has attempted to construct the pillar stress and roof-to-floor convergence profiles in order to evaluate the ultimate strength, deformation modulus, visco-elastic deformation, and violent failure characteristics of the pillar during longwall mining. This information reflects the overriding influence of the local geologic characteristics on bursts, provides the field measurements needed to verify concurrent modeling studies, and suggest some basic mechanisms associated with the coal pillar bursts discussed in this paper.

1 INTRODUCTION

Owing to the complex interaction of full-extraction techniques, overburden greater than 300-m (1000-ft), and unique geological characteristics, the Southern Appalachian Basin has had a long history of coal pillar burst problems. One of the earliest detailed reports on these occurrences was compiled by Rice (1935). This report identified numerous sites of fatal coal pillar bursts in Harlan County, Kentucky, and Wise County, Virginia. In one 4-month period eight miners were killed and a number injured by coal bursts.

Holland and Thomas (1954) examined 177 instances of pillar bursts, most of which were from the Southern Appalachian Basin, and found that the primary cause was unfavorable mining practices in abutment areas. Talman and Schroder (1958) emphasized the influence of very stiff overlaying strata on the occurrence of bursts in two different coalbeds in southern West Virginia, thereby confirming the importance of local geologic characteristics. Comprehensive laboratory and field data have been reported by Crouch and Fairhurst (1973) and Wang et al. (1976) on the properties of the Pocahontas #3 and #4 Coalbeds in West Virginia and Virginia. Campoli et al. (1987) documented the geologic, mining, and engineering parameters at five sites in West Virginia and Virginia where recent miner fatalities were associated with coal bursts.

Since most of these studies identified burst occurrences while slabbing and splitting pillars adjacent to large gobs during room and pillar mining, the potential for bursts in conjunction with longwall mining was anticipated. For this reason, the U.S. Bureau of Mines has been cooperating on joint field investigations with mine operators in Buchanan County, Virginia. These studies are obtaining the basic data necessary to optimize engineering designs in the hope of minimizing potential problems in the future.

2 GEOLOGIC CHARACTERISTICS OF THE STUDY SITE

Geological examinations and in-mine core drilling of the gate entries containing the study area have identified a 10-m thick, stiff siltstone (18 to 30 GPa Young's modulus) overlaying the coalbed (Figure 1). This unit is in turn overlain by a

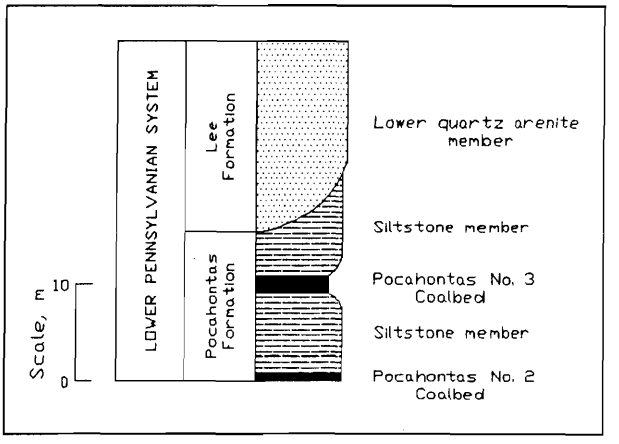

Figure 1. Stratigraphic section within the study area.

massive 40-m-thick quartz arenite sandstone. The coalbed floor consists of an equally stiff siltstone at least 10 m thick (Figure 1). Underground observations have indicated a persistent absence of prominent roof and floor fractures or joints. The main roof, dominated by the thick quartz arenite sandstone, is exceedingly difficult to break and complicates the use of general abutment load calculations, such as those identified by Mark (1987), to account for the extreme loads measured within the study area (see average stress calculations later in this paper).

3 PROPERTIES OF THE 24.4-M-SQUARE POCAHONTAS #3 COAL PILLAR

Perhaps the best way to begin an analysis of the behavior of pillars is to compare the 24.4-m (80-ft) square pillar with other pillars by using empirical pillar design formulae. This analysis will help to highlight problems with pillars having large width-to-height (W/H) ratios in burst-prone environments. This analysis will also emphasize the inability of the gate entry system to support the abutment loads at this site.

In determining a factor of safety for coal pillars 1.78-m (70-in) in height within the study area, it is first necessary to calculate the pillar loads generated during development mining. With an average overburden of 564 m (1850 ft), average development loads of 21.9 MPa (3180 psi) were calculated using the tributary area theory.

Empirical equations developed by Wang et al. (1976) and Bieniawski (1984) were used to determine a range of the ultimate strengths for the abutment pillar. Wang's equations were used in this analysis because they were based on actual in situ field test for the Pocahontas #3 Coalbed in West Virginia. The ultimate strength of a pillar is achieved when the pillar has reached its highest average stress. Once this point is achieved, the average pillar stress drops with a corresponding increase in pillar deformation, indicating the beginning of failure.

The ultimate strength of the abutment coal pillars was calculated at 19.5 MPa (2833 psi), assuming the strength for a 1.68-m (66-in) coal cube (Wang et al., 1976) of 5.2 MPa (758 psi). The W/H ratio [24.4-m / 1.78-m (80-ft / 5.83-ft)] of this pillar is 13.7. Using an alternate equation by Bieniawski, the ultimate strength of the abutment pillar was calculated at 28.4 MPa (4124 psi). It can be seen from these two values that the abutment pillars could have a safety factor of 0.9 or 1.3 after the development of the gate road entry system. This range of safety factors is of interest considering that Holland (1964) indicated that a pillar will probably become virtually indestructible when the W/H ratio exceeds 10. Yet, as is later shown, this pillar was able to withstand far higher stresses during longwall mining and eventually was destructible. Clearly, the empirical design formulae underestimate the strength of pillars with high W/H ratios.

Using an empirical method developed by Mark and Bieniawski (1986) called Analysis of Longwall Pillar Stability (ALPS), an accurate distribution of stresses within pillars in response to abutment loading can be determined. ALPS has the capability of estimating loads applied to the gate pillars, determining the pillar strength and load-bearing capacity, and calculating a "stability factor" for the entire gate entry design. The stability factor for the gate entry configuration at the study site was found to be less than 0.5. This estimate indicates sufficient loads were present to evaluate pillar behavior at and beyond its ultimate strength.

4 INSTRUMENTATION AND MINING METHOD

Evaluation of the behavior of the abutment pillar was accomplished by measuring pressure changes within and strata deformations around the coal. These observations were performed as the area was loaded during the extraction of the longwall panels on either side of the gate entries. A total of two abutment pillars and four yield pillars were instrumented with hydraulic coal cells in this study (Figure 2). Approximately 70 convergence stations were installed throughout the study area at the intersections and midpoints of every entry. Only a portion of the entire data set is discussed in this paper.

Throughout the length of the gate entries encompassing the study area, the abutment pillars were flanked on either side by 9.1-m (30-ft) yield pillars (Figure 2). With the arrival of the longwall face, these yield pillars crushed and ceased to be significant load bearing members. This statement is based on the performance of six coal cells placed across the width of 4 yield pillars and their adjacent convergence stations. The principal function of the yield pillar after failure was to serve as a protective barrier between a bursting

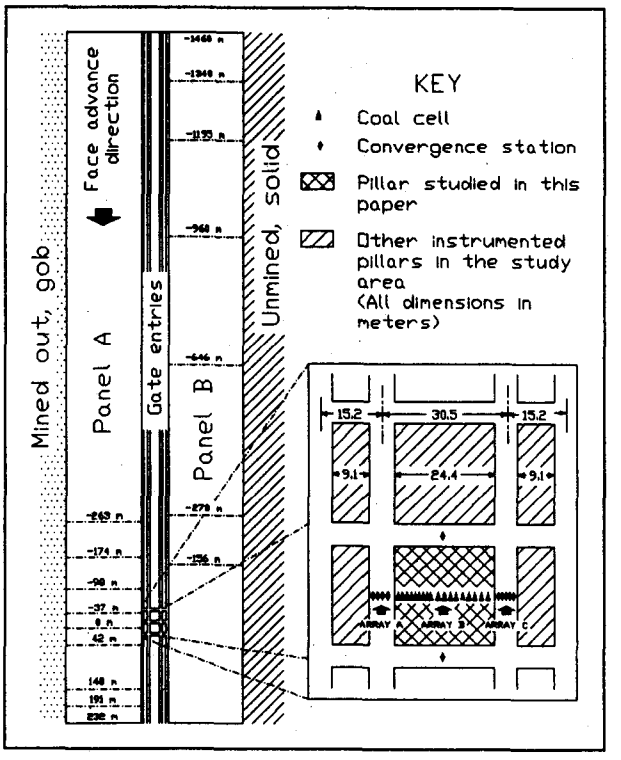

Figure 2. Layout of the mine around the abutment pillar and the location of the instruments used in this analysis.

abutment pillar and the longwall face. The 183-m (600-ft) wide longwall panels on either side of the gate road entries were the seventh and eighth in a series of east-west oriented mining areas (Figure 2).

The instruments used in this evaluation were 5-cm (2-in) diameter coal cells called Borehole Platen Flatjack (BPF) and convergence anchors measured with portable rods. The coal cell is a modified stainless steel hydraulic flatjack inserted between two aluminum platens (Bauer et al. 1985). The cells were set, three in one hole, at or near 17.2 MPa (2500 psi) and oriented to sense stress changes in the vertical direction. All 18 coal cells were set from 6 closely spaced drillholes (3 drillholes on either side of the pillar) across the width of the pillar. Convergence stations were set 0.91 m (3 ft) apart along this same trend in the entries on either side of the pillar.

All of the instruments were in place, and monitoring began when the longwall face of panel A was -263-m (-863-ft) away from the instrumented abutment pillar. (Note that - indicates in towards the face, and + out towards the mouth of the section.) Figure 2 shows the placement of the coal cell, array B, within the pillar and the roof-to-floor convergence arrays A and C in the entries with respect to the longwall panels (A and B). Because the hydraulic pressures measured from the coal cells represent an unrealistic value of pillar stress and because it was the purpose of this paper to analyze the average pillar stress and load, corrections to the readings of the coal cells were applied. The corrections applied to these pressure changes, herein referred to as cell calibration factor (CCF), have been the focal point of an exhausted laboratory and numerical modeling studies at the Bureau (Heasley 1989). The approach used in his analysis was to combine the analytical solution for the displacements around a borehole and the analytical solution for the borehole-platen interaction with

the empirical stiffness behavior of the flatjack. The resulting model of the BPF response has been verified using measured laboratory data with very good results. The CCF for each instrument was calculated based upon the individual fluid volume, length of tubing and coal properties. The stress values reported herewithin represent cell readings corrected by the above procedure.

5 PILLAR BEHAVIOR DURING LONGWALL MINING

Pillar stress change and strata convergence were analyzed to determine the ultimate strength and failure characteristics of the abutment pillar. These characteristics are important in determining the fundamental mechanism responsible for a burst and will be utilized in the future designs of mining systems for the Southern Appalachian Coal Basin. Assessment of the performance of the abutment pillar was achieved by examining the profiles of vertical stress distribution and the average stress across the pillar, and by examining the convergence in the adjacent entries. It should be noted that the average stress calculations were based on measuring the area under the profiles of the vertical stress distribution (Figures 3 and 4) and dividing this number by the pillar width.

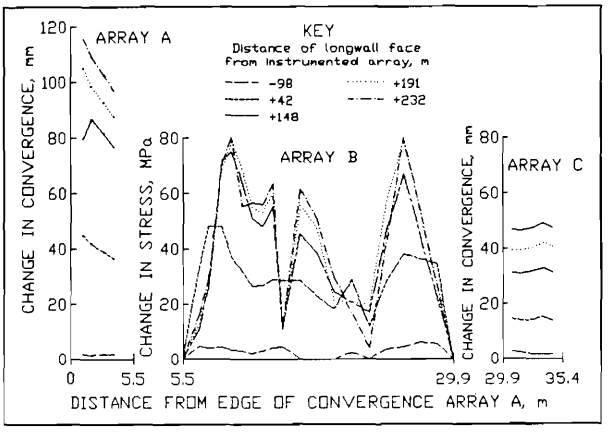

Figure 3. Detailed change in stress and convergence profiles from instrumented arrays A, B, and C during longwall face passage of panel A.

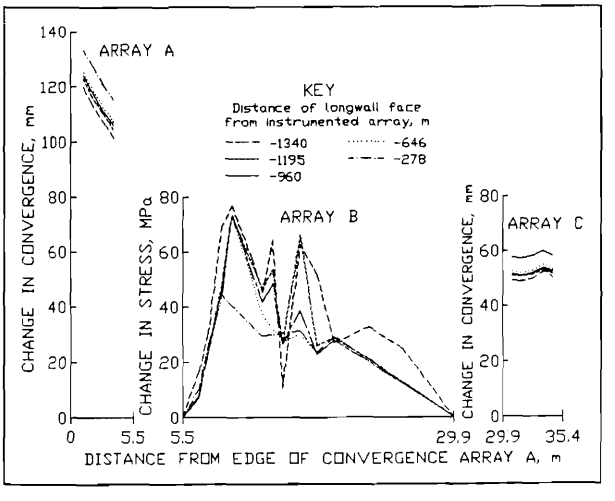

Figure 4. Detailed change in stress and convergence profiles from instrumented arrays A, B, and C during longwall face advance of panel B.

5.1 Detailed Stress and Convergence Profiles

In an attempt to better understand the distinct behavioral stages associated with the abutment pillar, detailed profiles of the individual stress and convergence changes are presented in Figures 3 and 4. Figure 3 shows the change in stress and convergence profiles from instrumented arrays A, B, and C (Figure 2) during the face passage of the panel A when the pillar load was rapidly increasing. The peak abutment stress first developed along the pillar edge and then migrated inward to about 3 to 3.7 m (9.8 to 12 ft). The coal from this peak stress zone to the outside edge of the pillar was highly fractured and is referred to as the "yield zone." The stresses in the pillar core were initially lower than the peak abutment stresses but rose dramatically as the ultimate strength of the pillar was approached. This pattern of behavior is very similar to Wagner's (1974) in situ test in South African coal mines using a "uniform deformation" loading system of coal pillars with a W/H ratio of 2. It is also interesting to note that the magnitudes of the peak abutment stresses remained constant after the initial rise suggesting the yield criteria proposed by Barron (1984) might apply to this case study.

Convergence measurements during this period of increased pillar load from array C (Figure 3) consistently measured a uniform closure rate across the 5.5-m (18-ft) span. It is clear that little or no roof bending took place and that the roof and floor rock were apparently acting as stiff plates. This conclusion is supported by the stress distribution profiles themselves and by the other convergence data located throughout the gate road entries. In array A, the roof-to-floor convergence profiles dip towards the yield pillar. Clearly the strata around the yield pillar and adjacent entries were breaking and rotating toward the newly formed gob in panel A. Observations of small fractures in the siltstone floor rock at the abutment pillar edge, separating the gate road into two distinctive loading environments, may possibly explain the uniform loading observed within the abutment pillar. It is assumed that only uniform convergence of the roof and floor over the abutment pillar could have produced symmetric stress profiles.

During the end of panel A face advancement {+191-m (+627-ft) to +232-m (+761-ft)}, little or no change in the stress profiles was observed (Figure 4), suggesting that pillar loads were nearly constant. However, beyond this point, peak abutment stresses remain virtually constant on the gob side of the pillar while stresses in the pillar core and the solid side of the pillar reduce significantly. It is difficult to rationally explain why the drop in pillar core stresses was not accompanied by a drop in the peak abutment stresses. Possibly, this trend is not "real" owing to the low number of operating coal cells; however, two horizontally oriented pressure cells placed 3-m (10-ft) and 9.1-m (30-ft) into the abutment pillar continued to measure significant horizontal confinement until the pillar began to burst at face position -156-m (-513-ft).

5.2 Change in Average Stress and Convergence

The average stress of the pillar was calculated at different longwall face positions from Figures 3 and 4. Calculation of the average stress is quite straightforward because of the high concentration of coal cells across the pillar. Note that the stress profiles are fairly symmetrical during the passage of the longwall face in panel A with the exception of face position +148-m (+485-ft). Calculation of average stress during the advance of the longwall face in panel B became more difficult as many of the cells on the right side of the pillar indicated zero stress. These zero stress conditions could have

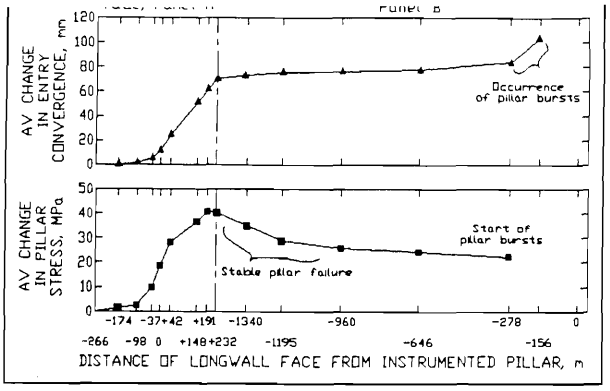

Figure 5. Average change in pillar stress and roof-to-floor convergence at various face positions of longwall panels A and B.

been a result of cell failure or local coal pillar failure. The statement that the ultimate strength of the pillar was exceeded and stable failure began was base upon the overall average stress calculations across the pillar, where clearly a drop in the stress level of the pillar core occurs. These values have been calculated as a means of defining the change in the behavior of the pillar from an unfailed to a failed state (Figure 5).

The abutment pillar was first affected by the advance of panel A (Figure 3 and 5) when the longwall face was about -150-m (-492-ft) away. As the face advanced, the stress and convergence both increased rapidly until panel A was mined out.

When the longwall face in panel B was started {-1460-m (-4790-ft)}, the average stress apparently began to decrease and the convergence continued at a slow but steady rate (Figure 5). Decreasing average stress continued until the face was at -960-m (-3150-ft), at which point the decrease in average stress moderated slightly. At the same time, roof-to-floor convergence continued at approximately the same rate.

There is only one obvious reason for the unloading of the pillar due to mining activity in and around panel B. From face position +191-m (+627-ft) to +232-m (+761-ft), the pillar was subjected to approximately constant loading with continuous deformation. This could have represented some type of visco-elastic behavior. From face position -1460-m (-4790-ft) to -278-m (-912-ft), the coal underwent stable pillar failure. During this stable failure, the pillar's load capacity reduced dramatically with continuing deformation. From face position -232-m (-912-ft) onward, the coal underwent a series of small burst.

The process described above, where pillar failure occurred during a stable loading period, may be analogous to creep failure in a laboratory test specimen as discussed by Goodman (1980). Figure 6 illustrates this principle where the failure occurred when a test sample, loaded to some critical stress level just below the ultimate strength, creeps until the accumulated strain intersects the falling part of the complete stress-strain curve. In applying this phenomena to coal pillars, the term visco-elastic deformation may be more appropriate.

5.3 Analysis of Pillar Deformation Modulus

Assuming that the roof-to-floor convergence measured adjacent to the instrumented pillar (Figure 2) were indicative of the pillar deformation, it is possible to plot the change in average pillar stress against

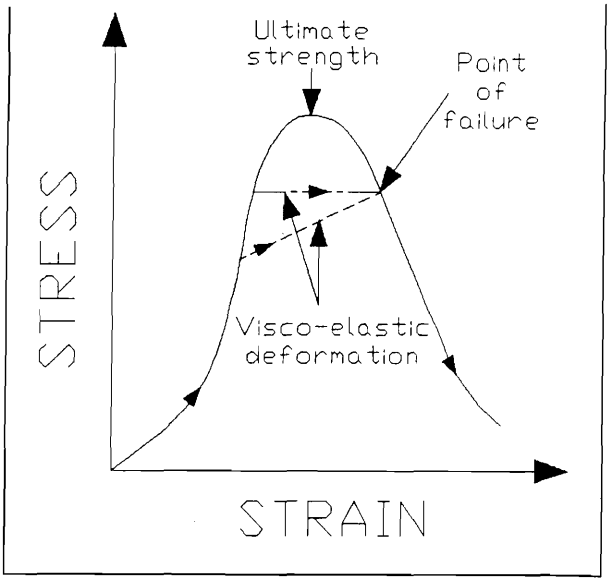

Figure 6. Creep in relation to the complete stress-strain curve (Goodman 1980).

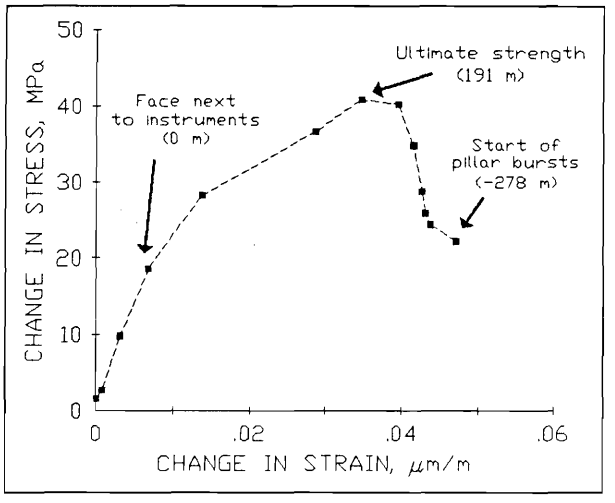

Figure 7. In situ stresss-strain curves for the Pocahontas #3 Coalbed as the pillar was loaded to failure.

the estimated pillar strain. Pillar strain was calculated by assuming the average pillar deformation was similar to the average entry deformation from array C (Figures 3 and 4) and dividing this average by the original coalbed height of 1.78-m (70-in). In fact the true pillar strain would be less than the average entry roof-to-floor convergence. However, for this analysis the shape of the curve would not change significantly if the average entry strain were multiplied by a fraction. Figure 7 shows the changes in slopes of the pillar stress-strain relationship as the coal is loaded to failure. This is very similar to the approach used by Wang et al. (1976) to evaluate the deformation modulus of a pillar in the Pocahontas #3 Coalbed of southern West Virginia.

During the face passage of panel A, the slope of the stress-strain curve gradually decreases (Figure 7). This decrease is most pronounced after the longwall face passes the instrumented array.

This apparently indicates an slight inelastic pillar response. The relatively higher pillar modulus as the longwall face is approaching the instrumented array may be related to the very rapid loading experienced during this time. With the completion of panel A and the beginning of panel B, the curve becomes almost flat, suggesting visco-elastic deformation under almost constant load. Beyond this point the slope becomes negative, indicating the pillar was in the post ultimate strength failure regime. This would appear to support the assumption that pillar failure occurred when the face of panel B was at or about -1460-m (-4790-ft) away from the pillar.

Analysis of the slopes of the stress-strain curve prior to the face passage of panel A (Figure 7) indicates a pillar deformation modulus of approximately 2.2 GPa (320,000 psi). Pillar deformation modulus calculations from data presented by Wang et al. (1976) averaged about 2.38 GPa (340,000 psi) and ranged between 2.07 and 2.76 GPa (300,000 and 400,000 psi). Wang et al. (1976) also determined that the average modulus from laboratory tests of this same coal to be 2.45 GPa (356,000 psi). The reader is advised to remember that these calculations are based upon entry deformations and not pillar deformations and that the modulus of the pillar is constantly changing in response to the proportions of yielded to solid (elastic to nonelastic) coal during pillar loading.

6 CHARACTERISTICS OF PILLAR BURSTS

The pillar began to bursts in a series of small events at a panel B face position of approximately -278-m (-911-ft). Unfortunately, by the time the longwall face of panel B had reached -156-m (-513-ft) from the abutment pillar, all but one of the coal cells had failed. The subsequent pillar behavior can therefore only be reported as based on visual observations. When the face of panel B had moved to within -156-m (-513-ft) of the pillar, the entire rib of the abutment pillar had sloughed off into the entry. Shortly after this, one side of the abutment pillar burst into the crosscut, partially closing it off (Figure 8). At this point, many of the other pillars between the instrumented abutment pillar and the longwall face were at least partially disintegrated. Additional bursting of the abutment pillar occurred at a face distance of -113-m (-371-ft). During this burst the crosscut closest to the face was totally closed off, while the other crosscut was partially closed off. Total disintegration of the pillar probably occurred at a face distance of -45-m (-148-ft). No further observation were made beyond this point.

Figure 8. View of the crosscut entry inby the abutment pillar when the longwall face from panel B was 159 m away.

Clearly, the bursts were initiated well after the pillar had passed its peak load bearing capacity. By the time the face was -278-m (-911-ft) away, approximately one-third of the load gained during panel extraction may have been shed from the pillar. Perhaps the most interesting observation made in this study (to the best of our knowledge the phenomenon has not been observed elsewhere) is the possibility that the pillars began to fail in a stable manner and did not burst for a considerable time after this failure began. Several scenarios that might explain the mechanism are postulated below.

7 MECHANISM FOR PILLAR BURSTS

Several hypothesis may be employed in speculating on the possible mechanism responsible for the coal pillar bursts discussed in this study. Certainly, the ability of coal to store high levels of elastic strain energy which can be suddenly released in the form of bursts was suggested by Holland and Thomas (1954) and has been greatly expanded on by many other researches. In the case of the pillar studied in this paper, it is difficult to know if any significant change in the levels of elastic strain energy occurred during the mining of the panel B, since the average stress appeared to decrease and the pillar deformation characteristics did not change until bursting began.

Another possible explanation for the coal bursts may be the sudden release in constraint between the coal pillar and the surrounding strata (e.g., slippage between the roof and/or floor and coalbed). Babcock and Bickel (1984) from the study of coal samples from 15 different mines, found that stress alone can produce bursts if constraint of the pillar was suddenly lost. This mechanism could be responsible for the bursts in this study, but actual existence of a change in the pillar constraint was not readily apparent.

A third hypothesis can be suggested as a possible mechanism that seems to fit the characteristics of this site well. As stated earlier, field data indicate that prior to bursting, the pillar was already following its post peak deformation curve. Salamon (1970) has demonstrated that, for a test specimen, equilibrium is maintained throughout the post peak force-displacement curve (the slope of which is called stiffness) up to the point at which the stiffness of the loading device becomes tangent to the curve (Figure 9). Salamon indicated that at

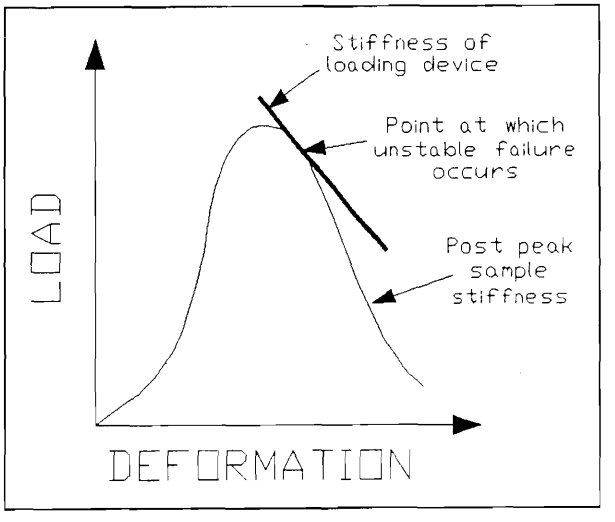

Figure 9. Criterion for test sample instability in terms of load-displacement relationships between the sample and the loading device (Salamon 1970).

this point in the test equilibrium would be interrupted by the dynamic yielding or violent failure of the specimen. (Equilibrium prevails only as long as the machine stiffness is greater than the sample stiffness.) Similarly, a pillar loaded beyond its ultimate strength, and following the downward portion of the post-peak curve, would continue to shed load and deform in a "stable" or steady manner until the post-peak curve intercepted the local mine stiffness curve. From this point onward, the stiffness of the pillar is greater than the stiffness of the mine, resulting in dynamic or unstable yielding of the coal pillar.

A fourth potential mechanism would be related to a dynamic stress wave generated from the abrupt failure of a large mass of rock or to the violent failure of an adjacent pillar. A sharp, instantaneous stress pulse applied to a highly stressed pillar could cause it to burst. Unfortunately, there does not appear to be any current way to prove or disprove any of the above mechanism with the field data available. However, these mechanisms supply useful insight into understanding the behavior of the pillar which is imperative if engineering designs are to successfully eliminate this hazard from our mines.

8 SUMMARY AND CONCLUSIONS

Using data gathered from borehole pressure cells and roof-to-convergence instrumentation, the behavior of a 24.4-m (80-ft) coal pillar prone to burst was investigated. The important characteristics of this behavior can be summarized as follows:

* As noted in many other studies, certain geological characteristics of the site must be present for a burst problem to occur. In this particular study, a moderately stiff siltstone overlain by an extremely stiff quartz arenite sandstone virtually free of fractures or joints appears to be a major factor influencing the occurrence of bursts.
* Empirical pillar strength and gate entry design formulations indicate the abutment pillar and the entry system in general had low safety "factors." These formulations provide evidence that the observed pillar should have been sufficiently loaded to fail prior to the passage of longwall panel B.
* The in situ pillar deformation modulus was estimated to be at least 2.2 GPa (320,000 psi) just prior to the passage of the longwall face in panel A.
* Post-peak pillar failure occurred not as the coal was loaded to its ultimate strength, but possibly after a short period of visco-elastic deformation. The pillar was thought to strain under constant load until it reached the downward side of the complete stress-strain curve, at which time pillar failure was initiated.
* Coal bursts did not occur until after the pillar had experienced significant steady disintegration or failure.
* Possible explanations for mechanism responsible for the pillar bursts observed in this study are excessive elastic levels of strain energy in the pillar core, a change in pillar constraint at the coalbed interfaces, the sudden existence of a condition where the pillar stiffness is in excess of the surrounding mine stiffness, and the instantaneous application of a dynamic stress pulse. All of these mechanism may have promoted violent failure of the pillar.

9 ACKNOWLEDGEMENTS

The work described in this paper is part of an extensive investigation carried out by the U.S. Bureau of Mines to design mining system that will reduce the occurrence of bursts in coal mines. The author is extremely grateful to all of his colleagues at the Pittsburgh and Denver Research Centers and to Dr. Barron a visiting professor from the University of Alberta who have provided many stimulating discussions on the subject and have shown great patience in the process.

REFERENCES

Babcock, C.O. and D.L. Bickel 1984. Constraint - The Missing Variable in the Coal Burst Problem. Proc. 25th U.S. Symp. on Rock Mech., Evanston, IL, pp. 639-647.

Barron, K. 1984. An Analytical Approach to the Design of Coal Pillars. CIM Bulletin, August, pp. 37-44.

Bauer, E.R., G.J. Chekan, and J.L. Hill, Jr. 1985. A Borehole Instrument for Measuring Mining-Induced Pressure Changes in Underground Coal Mines. Proc. 26th U.S. Symp. on Rock Mech., Rapid City, SD, pp. 1075-1084.

Bieniawski, Z.T. 1984. Rock Mechanics Design in Mining and Tunneling. A.A. Balkema, Rotterdam, Netherlands, pp. 197-209.

Campoli, A.A., C.A. Kertis, and C.A. Goode 1987. Coal Mine Bumps: Five Case Studies in the Eastern U.S. U.S. Bureau of Mines IC 9149, 34 pp.

Crouch, S.L. and C. Fairhurst 1973. The Mechanics of Coal Mine Bumps and the Interaction Between Coal Pillars, Mine Roof, and Floor, U.S. Bureau of Mines Contract Report H0101778, Feb., 88 pp.

Goodman, R.E. 1980. Introduction to Rock Mechanics. John Wiley & Sons, New York, pp. 74-75.

Heasley, K.A. 1989. Understanding the Hydraulic Pressure Cell. Proc. 30th U.S. Symp. on Rock Mech., Morgantown, WV, in press.

Holland, C.T. 1964. The Strength of Coal in Mine Pillars. Proc. of the 6th Symp. on Rock Mech., Rolla, MO, pp. 450-466.

Holland, C.T. and E. Thomas 1954. Coal-Mine Bumps: Some Aspects of Occurrence, Cause, and Control. U.S. Bureau of Mines Bulletin 535, 37 pp.

Mark, C. 1987. Analysis of Longwall Pillar Stability. PhD Thesis, Pennsylvania State University, State College, PA, pp. 8-24.

Mark, C. and Z.T. Bieniawski 1986. An Empirical Method for the Design of Chain Pillars for Longwall Mining. Proc. 27th U.S. Symp. on Rock Mech., Tuscaloosa, AL, pp. 415-422.

Rice, G.S. 1934. Bumps in Coal Mines of the Cumberland Field, Kentucky and Virginia--Causes and Remedy. U.S. Bureau of Mines RI 3267, 36 pp.

Salamon, M.D.G. 1970. Stability, Instability and Design of Pillar Workings. Int. J. Rock Mech. Min. Sci., Vol. 7, pp. 613-631.

Talman, W.G., and J.L. Schroder, Jr. 1958. Control of Mountain Bumps in the Pocahontas #4 Seam. Transactions of the A.I.M.E., pp. 888-891.

Wagner, H. Determination of the Complete Load-Deformation Characteristics of Coal Pillars. Proc. 3rd. Int. Cong. on Rock Mech., ISRM, Denver, pp. 1076-1081.

Wang, F.D., W.A. Skelly, and J. Wolgamott 1976. In Situ Coal Pillar Strength Study. U.S. Bureau of Mines Contract Report #H0242022, 110 pp.